**Egyptian Journal of Geology**

**https://egjg.journals.ekb.eg**

# Characterization of some Um Bogma manganese ores in Um Bogma area and their potentiality for upgrading and manufacturing of manganese alloys

**Ahmed G. Moustafa[1], Nagui A. Abdel-Khalek[2], Ahmed A. Sharaf-Eldin[1], Abdelmonem M. Soltan[1]** and **El-Sayed R. E. Hassan[2]**

[1] *Geology Department, Faculty of Science, Ain Shams University, Abbassia, 11566, Cairo, Egypt*
*https://orcid.org/0000-0002-7546-2854*

[2] *Minerals Beneficiation and Agglomeration Department, Minerals Technology Division, Central Metallurgical Research & Development Institute (CMRDI), P.O. Box 87 Helwan, 11722 Cairo, Egypt*

The textural, mineral, and chemical composition as well as thermal behaviour of technological samples representing Um Bogma manganese ore in Um Bogma area were investigated using several lab techniques. The obtained results were used to assess their potentiality for upgrading and production of manganese alloys. Pyrolusite and, in a few cases, manganite are the essential manganese minerals. These are associated with varying proportions of hausmannite, hematite, goethite, and quartz. The chemical composition data confirm well with those of mineralogy. The ore samples display various textural patterns in which the essential Mn and Fe minerals have different modes of occurrence. Combining the various characteristics of the manganese ore samples indicates that some are amenable for upgrading and beneficiation.

**Keywords:** Sinai, Um Bogma area, Mn ores, grades and beneficiation.

## 1. Introduction

Manganese is an essential alloying element in nearly all types of steel and is used to increase their strength, toughness, hardness, and hardenability (Singh et al., 2020). Manganese is used for deoxidation and desulphurisation of ferrous metals and alloys and the production of ferromanganese and silicomanganese alloys for steel/iron manufacturing and cast iron (Fahim et al., 2013; El-Hussiny et al., 2016). Pure manganese (produced electrolytically) is utilized mostly in the preparation of nonferrous alloys of copper, aluminium, magnesium, and nickel and in the production of high-purity chemicals (Singh et al., 2020). Also, Mn oxides are used in the production of manganous salts or as an additive in fertilizers, a reagent in textile printing, chemical oxidant in organic synthesis, and as the cathode material in dry-cell batteries ((Tan et al., 2004; Liu et al., 2019; and El Aref et al., 2020).

Concentration of Mn oxides of different geologic settings and variable economic values exist in several localities in Egypt (El Aref et al., 2020; **Fig. 1**) include: Sinai (Um Bogma region; Sharm El Sheikh), Eastern Desert (Wadi Araba, East Ras-Zafarana, Wadi Bali, Gabal Abu Shaar, Ech Elmalaha, W Meialeik, Halaib-ElBa region), and Western Desert (El Bahariya oasis).

Um Bogma area in west-central Sinai is regarded as one of the main sources of the Egyptian manganese ore (Salem et al., 2016; El Aref et al., 2020) with around 1.7 million tons ore reserve. (Fahim et al., 2013; **Fig. 1**). These manganese ores are of low grade and have Mn/Fe < 5 (Tan et al, 2004). The manganese ore is extracted by Sinai Manganese Company (SMC) and fed directly into the industrial kiln without beneficiation for manufacturing of silicon-manganese and ferromanganese alloys by mixing with either imported high grade Mn ore or Mn sinter to increase the Mn/Fe ratio of the kiln feed.

*Corresponding author e-mail: ahmedgamal@sci.asu.edu.eg
Received: 05/05/2024; Accepted: 05/06/2024
DOI: 10.21608/EGJG.2024.287498.1076

In Um Bogma area, the manganese ore is found in Um Bogma Formation, which represents a carbonate succession of Early Carboniferous age (Kora et al., 1994; Shaaban et al., 2005; El-Anwar, 2014; and Kordi et al., 2017). It occurs as stratiform ore bodies present within shale beds (El-Shafei et al., 2022). Many literatures discussed the genesis of Um Bogma Manganese ore. Some studies concluded a hydrothermal origin (Gindy, 1961; Nakhla and Shehata, 1963; Saad et al., 1994; Khalifa and Seif, 2014; and El-Shafei et al., 2022), whereas others lean to a sedimentary origin (Mart and Sass, 1972; Magaritz and Brenner, 1979; Kora 1984; and ElAgami et al., 2000).

The manganese ore of Um Bogma is classified as ferruginous Manganese ore, in which pyrolusite and hematite are the essential minerals. It has varying chemical composition/grade. (El Shazly and Saleeb, 1959; Fahim et al., 2013; and El-Shafei et al., 2022).

The present work primarily focuses on the examination of the mineral, chemical, and textural attributes of the run-of-mine samples sourced from Sinai Manganese Company (SMC). This examination aims to assess the feasibility of applying mineral processing methods on these samples.

## 2. Materials and Methods

### 2.1 Materials

Four run-of-mine technological samples representing the manganese ore from Um Bogma area were collected. It should be mentioned that SMC extracts the ores from Um Bogma mines and classifies them into four different grades according to their chemical characteristics.

### 2.2 Methods

**X-ray diffraction (XRD) analysis** was conducted to identify the mineral phases in the studied samples. This was achieved by using Panalytical X'Pert PRO XRD device at the Technical Institute, George Simon Ohm, Germany. The obtained data were interpreted by using "Match" software.

**Fourier-transform infrared spectroscopy (FTIR)** was conducted by using Bruker Alpha 2 FTIR spectrometer.

**Thermogravimetric analysis (TGA)** was performed to determine the thermal behavior. The analysis was performed by using Shimadzu TGA 50 device.

**X-ray fluorescence analysis (XRF)** was conducted to determine the chemical composition of the manganese ore samples by using PANalytical Axios XRF spectrometer at the Technical Institute, George Simon Ohm, Germany.

**Polished sections** of the manganese ore samples were prepared and examined by reflected light using Olympus microscope. Portugal) attached with a camera and PC Olympus workspace software. The polished sections were studied for mineralogical and textural chrematistics of the manganese samples.

**Scanning electron microscopy (SEM)** was carried out on the studied manganese ore samples by using SEM attached with EDX module and PC software at the NTRC unit, SEM lab at the British University in Egypt.

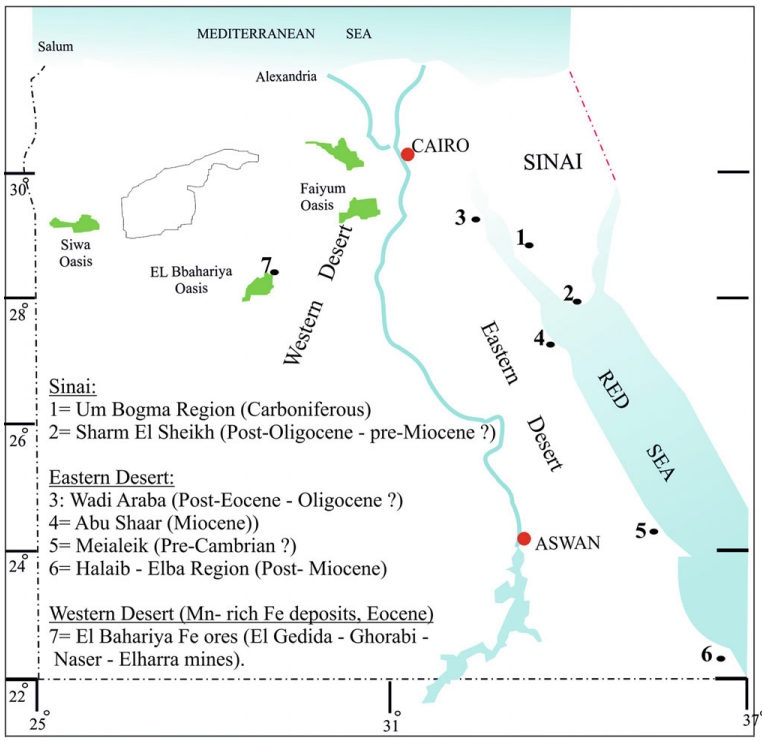


**Fig. 1. Localities of Mn ores in Egypt (El Aref et al., 2020).**

## 3. Results and Discussion

### 3.1. Mineralogical studies

**Fig. (2)** presents the X-ray diffraction patterns of the manganese ore samples. The semi-quantitative percentages of the recorded minerals are given in **Table (1)**.

Samples (1), (2), and (3) contain pyrolusite ($MnO_2$, Card no. 96-901-5695) as a major Mn mineral (47.8, 26, and 85.9 % respectively). Hausmannite ($Mn^{2+}Mn^{3+}{}_2O_4$, Card no. 96-101-1263) is present in sample 2 (18.5 %) while manganite {MnO (OH), Card no. 96-901-6547} is the secondary manganese mineral in sample 3 (4.1 %). Unlike the previous three samples, the XRD chart of sample 4 shows that the main manganese mineral is manganite {MnO (OH), PDF no. 96-901-6547; 66.7%}, it is followed by pyrolusite ($MnO_2$, Card no. 96-901-5695; 26.9 %). The main iron mineral in all samples is hematite ($Fe_2O_3$, Card no. 96-900-0140; 24.2, 22.3, 10, and 6.5 % respectively), whereas goethite {FeO (OH), Card no. 96-902-5697} exists only in samples (1) and (2) (17.6 and 17.1 % respectively). Quartz ($SiO_2$, Card no. 96-900-5019) represents the only non-metallic mineral. It exists in samples (1) and (2) (10.4, and 16 % respectively).

The interpreted mineralogic content in this study is quite similar to the findings of Fahim et al (2013), Abd El-Gawad et al, (2014), and El-Hussiny et al. (2016) which concluded that the essential minerals of Um Bogma manganese ore are pyrolusite, hematite, and quartz.

### 3.2. Fourier-transform infrared spectroscopy (FTIR):

The FTIR charts of the studied technological manganese ore samples are shown in **Fig. (3**). The presence of pyrolusite is confirmed by its characteristic absorbance peak at 558cm$^{-1}$. Hematite in all samples shows its characteristic two absorbance peaks at 532cm$^{-1}$ and 647cm$^{-1}$, the former peak overlaps with the characteristic peak of pyrolusite. The three absorbance peaks at 1085cm$^{-1}$, 1114cm$^{-1}$, and 1150cm$^{-1}$ refer to manganite, which is the essential manganese mineral in sample (4) and an accessory mineral in sample (3). Goethite in samples (1) and (2) shows its characteristic peaks at 593cm$^{-1}$, 890cm$^{-1}$, and 910cm$^{-1}$. The absorbance peaks in the range 1200 – 4000cm$^{-1}$ correspond to the O-H bond of the free water (moisture) and the connate hydroxides of the mineral phases (Chukanov, 2014).

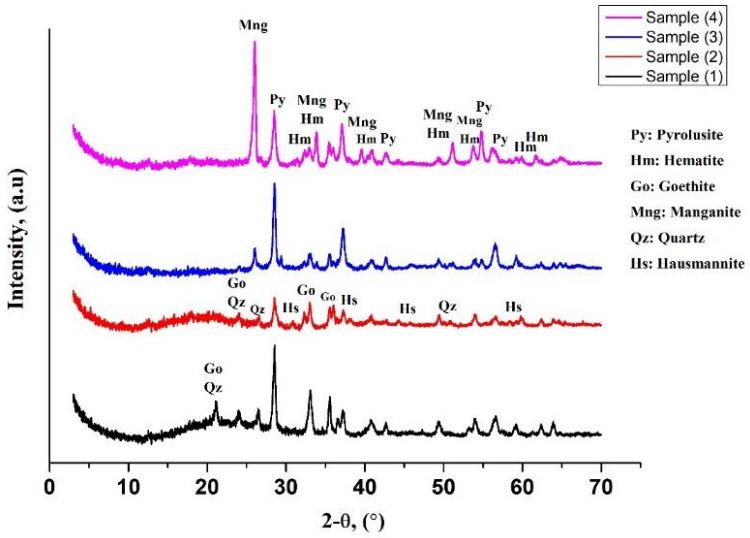


**Fig. 2. XRD charts for the technological manganese ore samples.**

**Table 1. Semi-quantitative percentages of the main minerals of the studied manganese ore samples.**

| Mineral / Sample | Pyrolusite | Hausmannite | Manganite | Hematite | Goethite | Quartz |
|---|---|---|---|---|---|---|
| **Sample 1** | 47.8 | - | - | 24.2 | 17.6 | 10.4 |
| **Sample 2** | 26 | 18.5 | - | 22.3 | 17.1 | 16 |
| **Sample 3** | 85.9 | - | 4.1 | 10 | - | - |
| **Sample 4** | 26.9 | - | 66.7 | 6.5 | - | - |

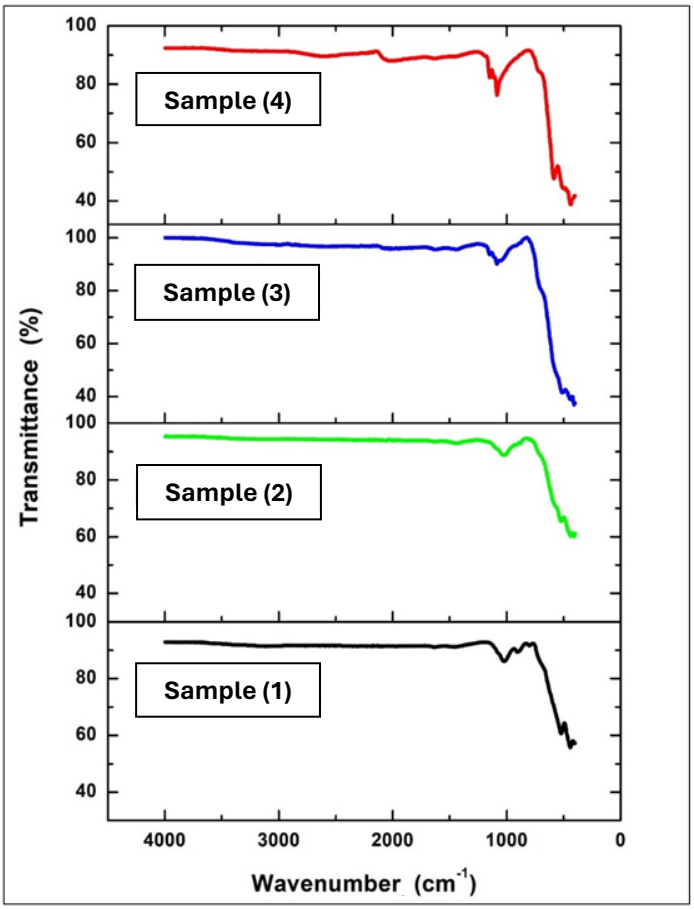


**Fig. 3. FTIR spectra of the technological manganese ore samples.**

### 3.3. Thermal behaviors:

The TGA charts of the manganese ore samples are shown in **Figs. (4 to 7**). In each of these charts, the first weight loss (below 200°C) frequently represents the evaporation of free water (Long et al., 2015). The sequential transformation and decomposition reactions for all the mineral phases that exist in the studied samples were discussed by Földvári (2011) as follows:

1- The endothermic equation of the manganite of MnO(OH) → $Mn_2O_3$ occurs at 350-400°C.

2- The endothermic peaks of pyrolusite that represent the reduction equation $MnO_2$ → $Mn_2O_3$ is frequently located at the temperature range 625-725°C.

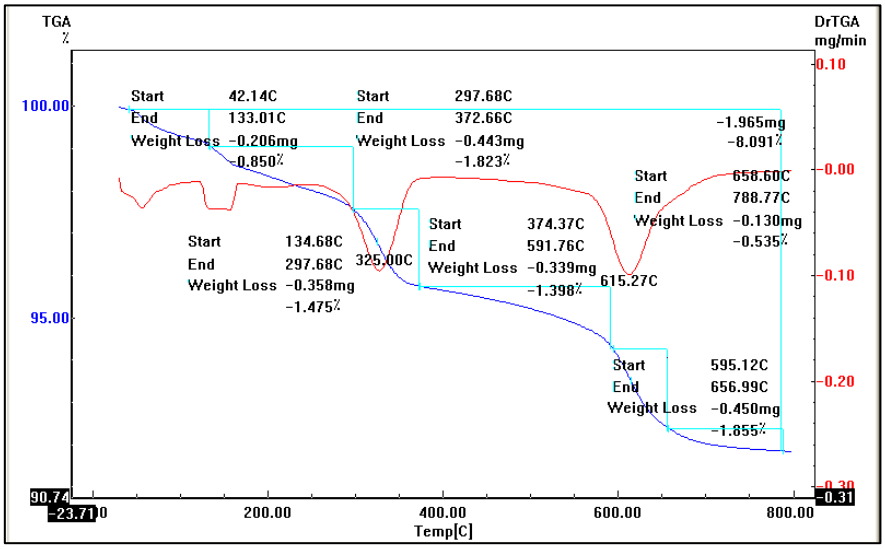


**Fig. 4. TGA curve and its derivative of technological manganese ore sample (1).**

3- The decomposition reaction $Mn_2O_3$ → $Mn_3O_4$ usually occurs at the range 700-800°C (Song et al., 2023).

4- The transformation of goethite to hematite ($FeO(OH)$ → $Fe_2O_3+H_2O$) is located at temperature range 290-330°C.

5- The characteristic endothermic peak of hematite (Curie-point) appears at 675-680°C.

6- The distinct structural transition of quartz (trigonal → hexagonal) is represented by endothermic peak at 573°C.

**Table (2)** summarizes the interpretation of the TGA charts of the four manganese ore samples (**Figs. 4 to 7**) integrated with other analyses interpretations with mentioning all the presented peaks with their equivalent reactions. Some peaks of different minerals overlap with each other.

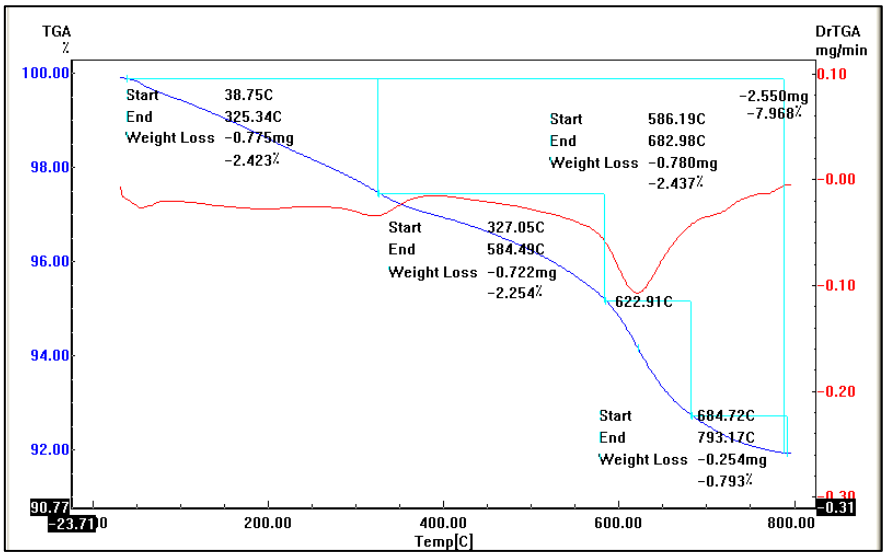


**Fig. 5. TGA curve and its derivative of technological manganese ore sample (2).**

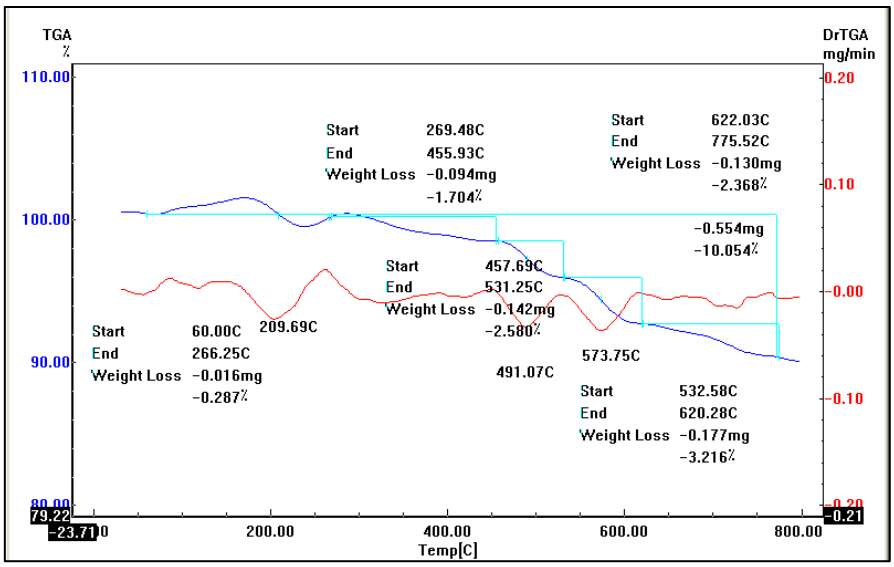


**Fig. 6. TGA curve and its derivative of technological manganese ore sample (3).**

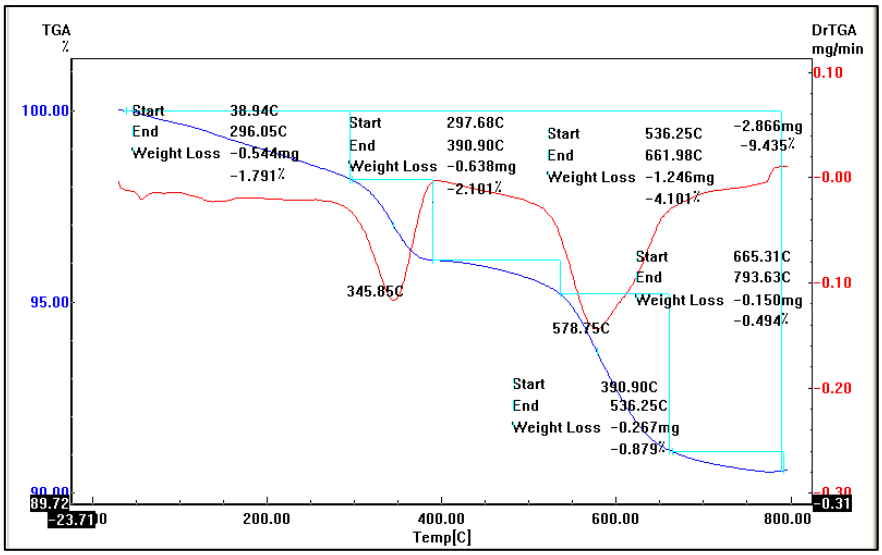


**Fig. 7. TGA curve and its derivative of technological manganese ore sample (4).**

**Table 2. TGA data for the technological manganese ore samples.**

| Sample | Temperature (ºC) | Weight loss (%) | Total loss (%) | Transformation reaction |
|---|---|---|---|---|
| **1** | 42.14 – 133.01° C<br>134.68 – 297.68° C<br>279.68 – 372.66° C<br>374.37 – 591.76° C<br>595.12 – 656.99° C<br>658.6 – 788.77° C | 0.85 %<br>1.475 %<br>1.823 %<br>1.398 %<br>1.855 %<br>0.535 % | 8.091 % | Free water and volatiles<br>Free water and volatiles<br>Goethite {FeO (OH)) → $Fe_2O_3$}<br>Quartz (trigonal → hexagonal)<br>Pyrolusite ($MnO_2$ → $Mn_2O_3$)<br>Hematite + ($Mn_2O_3$ → $Mn_3O_4$) |
| **2** | 38.75 – 325.34° C<br>327.05 – 584.49° C<br>586.19 – 682.98° C<br>684.72 – 793.17° C | 2.423 %<br>2.254 %<br>2.437 %<br>0.793 % | 7.907 % | Free water and volatiles<br>Goethite {FeO (OH)) → $Fe_2O_3$} + Quartz<br>Pyrolusite ($MnO_2$ → $Mn_2O_3$)<br>Hematite + ($Mn_2O_3$ → $Mn_3O_4$) |
| **3** | 60 – 266.25° C<br>269.48 – 455.93° C<br>457.69 – 531.25° C<br>532.58 – 620.28° C<br>622.03 – 775.52° C | 0.287 %<br>1.704 %<br>2.58 %<br>3.216 %<br>2.368 % | 10.155 % | Free water and volatiles<br>Manganite {MnO(OH)) → $Mn_2O_3$}<br>Manganite {MnO(OH)) → $Mn_2O_3$}<br>Pyrolusite (MnO2 → $Mn_2O_3$)<br>Hematite + ($Mn_2O_3$ → $Mn_3O_4$) |
| **4** | 38.94 – 296.05° C<br>297.68 – 390.90° C<br>390.90 – 536.25° C<br>536.25 – 661.98° C<br>665.31 – 793.63° C | 1.791 %<br>2.101 %<br>0.879%<br>4.101 %<br>0.494 % | 9.366 % | Free water and volatiles<br>Manganite {MnO(OH)) → $Mn_2O_3$}<br>Manganite {MnO(OH)) → $Mn_2O_3$}<br>Pyrolusite ($MnO_2$ → $Mn_2O_3$)<br>Hematite + ($Mn_2O_3$ → $Mn_3O_4$) |

### 3.4. Geochemical studies

**Table (3)** presents the chemical composition data for the studied samples. It shows that MnO (33.93 – 69.37 wt.%) and $Fe_2O_3$ (11.39 – 44.07 wt.%) are the major oxides. The enrichment of sample (1) in $Fe_2O_3$ (44.07 wt.%) is attributed mainly to the dominance of hematite (24.2 %; **Fig. 2 and Table 1**). On the other hand, MnO is the major oxide in samples 2, 3, and 4 (55.4 - 69.37 wt.%) in which the $Fe_2O_3$ contents range from 11.39 to 21.68 wt.%. This could be interpreted based on the enrichment of samples (2) and (3) in pyrolusite (26 and 85.9% respectively; **Fig. 2 and Table 1**), in addition to the enrichment of sample (2) in hausmannite ($Mn^{2+}Mn^{3+}{}_2O_4$) and sample (4) in manganite {MnO(OH)} as well as pyrolusite ($MnO_2$)

and manganite {MnO(OH)} in sample (3) (18.5 and 4.1 % respectively, **Fig. 2 and Table 1**).

In general, the existence of high percentage of iron in Um Bogma manganese ore is expected, as it is a ferruginous ore type (Kordi et al., 2017; Araffa et al., 2020; and El-Shafei et al., 2022). The MnO contents in the samples are in sample 1 (33.93 wt.%), sample 3 (55.4 wt.%), sample 2 (55.55 wt.%), and sample 4 (69.37wt.%). The concentrations of $Fe_2O_3$ are in the reverse order (**Table 3**) which was explained in Fahim et al. (2013).

The significant existence of $SiO_2$ in samples (1) and (2) (6.18 and 7.9 wt.%; respectively) is attributed to the presence of considerable concentrations of quartz (10.4 and 16 %; respectively; **Fig. 2 and Table 1**). According to Johnson and Mccartney (1965), the manganese ores could be classified based on the Mn contents into iron ores (having Mn contents less than 5%), manganiferous iron ores (in which Mn contents range from 5 to 35 wt.%; sample 1), and manganese ores (that have Mn content more than 35%; samples 2, 3, and 4).

**Table 3. Chemical composition of the studied technological manganese ore samples.**

| *Classification* | **Manganiferous iron ore** | **Manganese ore** | **Manganese ore** | **Manganese ore** |
|---|---|---|---|---|
| *% Assay (as oxides)* | **Sample (1)** | **Sample (2)** | **Sample (3)** | **Sample (4)** |
| **MnO** | 33.93 | 55.55 | 55.4 | 69.37 |
| **$Fe_2O_3$** | 44.07 | 20.93 | 21.68 | 11.39 |
| **$SiO_2$** | 6.18 | 7.09 | 2.52 | 2.57 |
| **$Al_2O_3$** | 2.27 | 1.48 | 0.67 | 0.73 |
| **CaO** | 1.82 | 1.93 | 1.98 | 0.56 |
| **$Na_2O$** | 0.18 | 0.16 | 0.16 | 0.12 |
| **MgO** | 0.92 | 1.36 | 0.47 | 0.72 |
| **$K_2O$** | 0.25 | 0.26 | 0.35 | 0.16 |
| **BaO** | 0.76 | 0.8 | 0.52 | 1.77 |
| **Cl** | 0.2 | 0.06 | 0.11 | 0.06 |
| **$SO_3$** | 0.23 | 0.2 | 0.38 | 0.93 |
| **LOI** | 8.35 | 8.84 | 12.25 | 10.64 |
| ***As % Metal*** | | | | |
| **Mn%** | 26.26 | 43.00 | 42.88 | 53.69 |
| **Fe%** | 30.80 | 14.63 | 15.15 | 7.96 |
| **Mn/Fe ratio** | 0.85 | 2.94 | 2.83 | 6.74 |

### 3.5 Ore microscopic studies

The examination of the polished sections of the manganese ore samples by using RLM, which is based on Pracejus (2015), shows that the main manganese mineral is pyrolusite ($MnO_2$). It appears in yellowish to yellowish/greyish tint white color and has moderate to high reflectance (**Figs. 8 to 10**). In sample (4), the identified manganese mineral is

manganite {MnO (OH)} which displays a medium grey color and has a high reflectance (**Fig. 11**).

The texture of sample (1) consists of microcrystalline manganese grains disseminated among iron oxide particles represented by light bluish grey hematite and grey with bluish tint goethite together with other black gangue minerals (mainly quartz) (**Fig. 8**).

The disseminated texture indicates high difficulty in the ability of ore processing (Craig and Vaughan, 1994).

On the other hand, the textures of samples (2), (3), and (4) consist of polygonal, non-equant to equant/prismatic manganese patches set in groundmass made up of iron oxides and quartz (**Figs. 9 to 11**).

This implies that these samples have larger possibility of processing than sample (1) because of its disseminated. Also, sample (3) has almost regular distribution of manganese patches -with average diameters ranging between 250 and 500 µm- among a groundmass made up of iron oxides and other gangue minerals (**Fig. 10**). This textural pattern facilitated the estimation of the mineral liberation size as an essential step in processing procedures (Craig and Vaughan, 1994).

**3.6. Microchemical studies:**

The SEM examination supported with EDX analysis of the studied technological manganese ore samples (1), (2), (3), and (4) (**Figs. 12, 13, 14, and 15**; respectively) revealed the presence of different micro regions of various contrasts. Those having creamy grey color represent manganese minerals (pyrolusite and manganite) whereas areas with darker grey color correspond to the iron minerals (hematite and goethite).

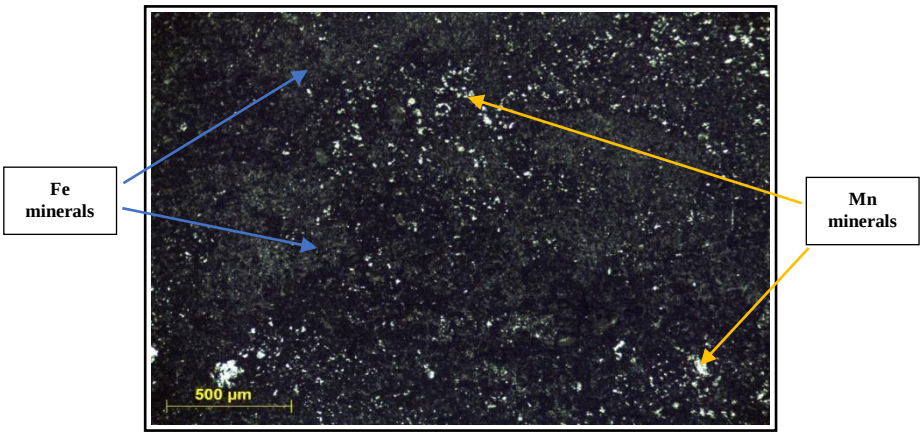


**Fig. 8. Photomicrograph of sample (1) showing yellowish white microcrystalline manganese particles disseminated in a groundmass composed of iron oxides and other gangue minerals (RLM).**

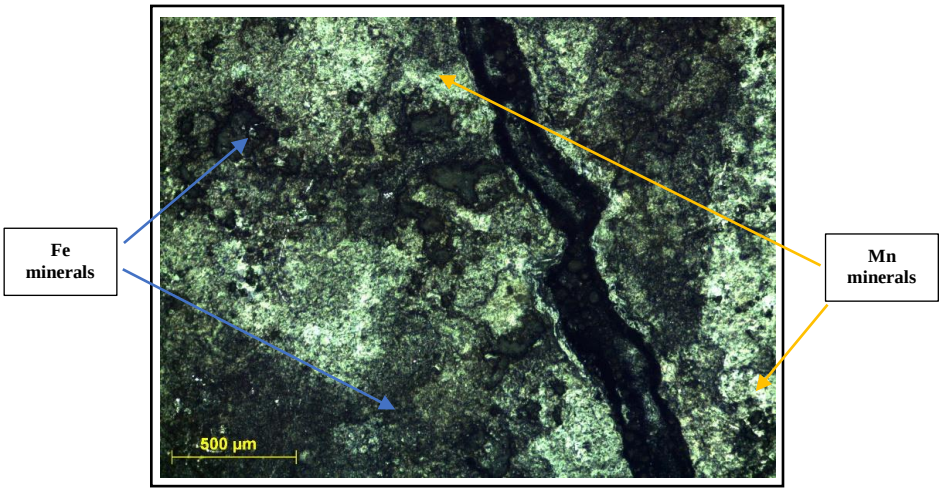


**Fig. 9. Photomicrograph of sample (2) showing yellowish white manganese patches together with iron oxides and other gangue minerals patches (RLM).**

Crystals of the manganese minerals have different morphologies.

In sample (1), pyrolusite exists in the form of colonies of columnar prismatic crystals (**Fig. 12a**). In samples (1), (2), and (3), pyrolusite exists as radial fibrous and acicular crystals (**Fig. 12a, Fig. 13b, Figs. 14a, b, and c;** respectively).

Manganite occurs as colonies of prismatic crystals in sample 4 (**Figs. 15a and b**). Hematite appears as pseudo-cubic and platy tabular crystals in sample (1) (**Figs. 12b and 6c**) and as prismatic crystals in sample 2 (**Fig. 13a**). Quartz occurs as dense grains with light grey contrast in sample 2 (**Fig. 13a**).

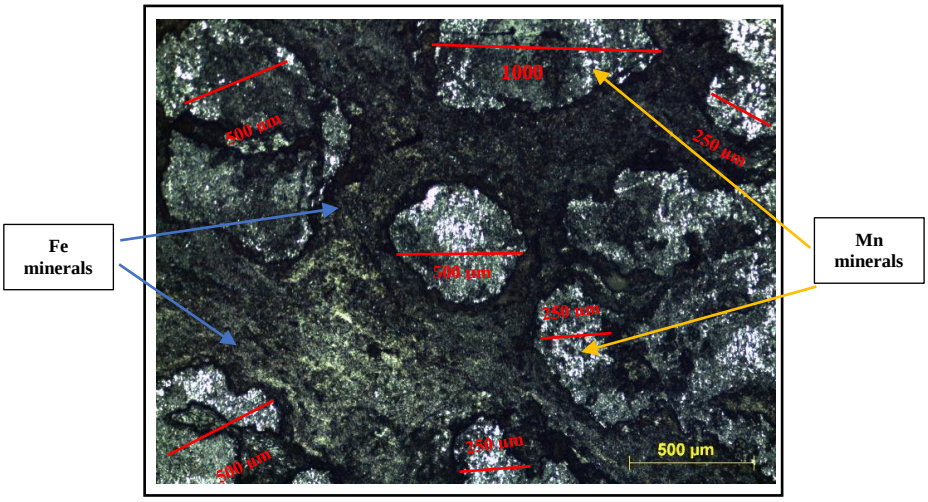


**Fig. 10. Photomicrograph of sample (3) showing yellowish/greyish white manganese particles having equant-prismatic shape and approximately similar dimensions that are set in a groundmass made up of iron oxides and other gangue minerals (RLM).**

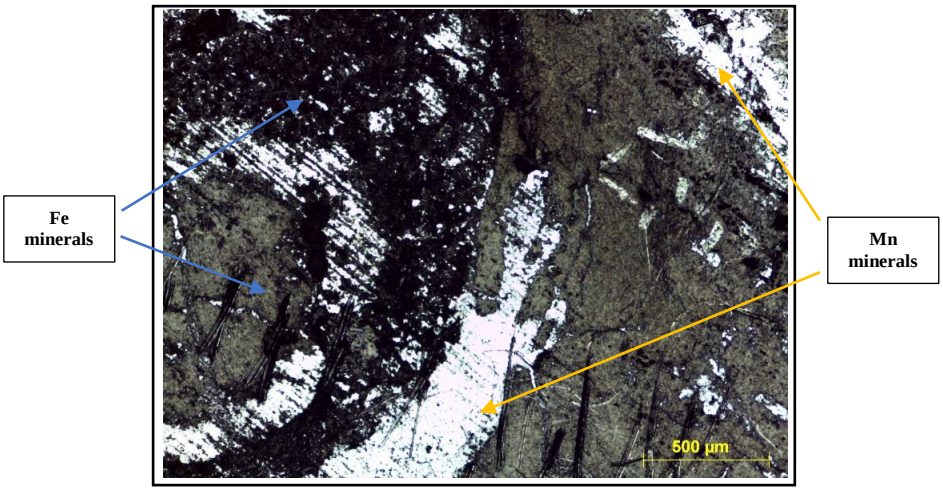


**Fig. 11. Photomicrograph of sample (4) showing medium grey patches of manganese oxides randomly distributed among other iron oxides and gangue minerals (RLM).**

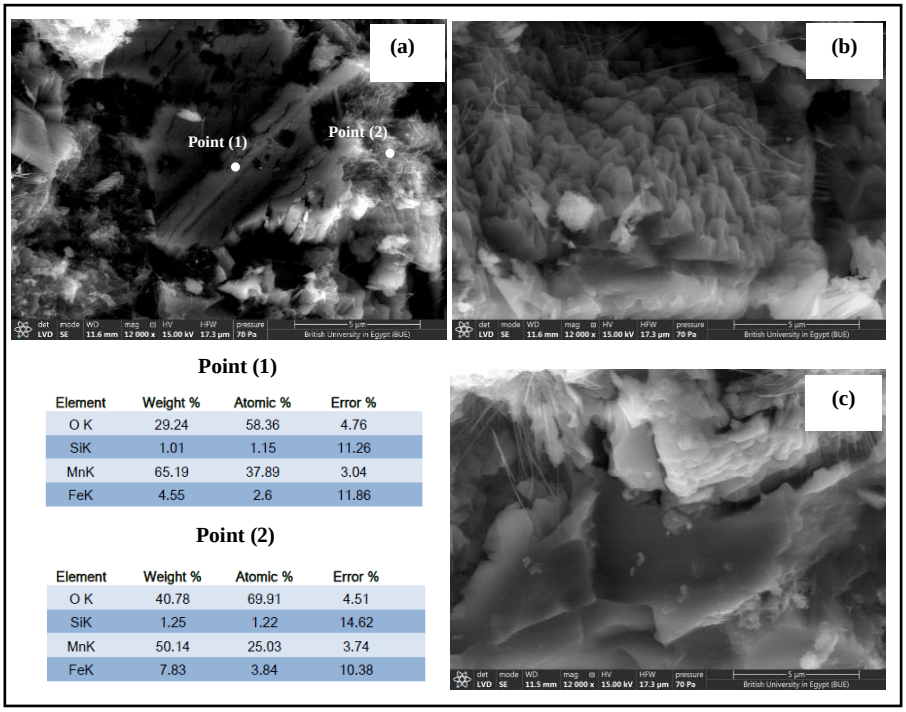


**Point (1)**

| Element | Weight % | Atomic % | Error % |
|---|---|---|---|
| O K | 29.24 | 58.36 | 4.76 |
| SiK | 1.01 | 1.15 | 11.26 |
| MnK | 65.19 | 37.89 | 3.04 |
| FeK | 4.55 | 2.6 | 11.86 |

**Point (2)**

| Element | Weight % | Atomic % | Error % |
|---|---|---|---|
| O K | 40.78 | 69.91 | 4.51 |
| SiK | 1.25 | 1.22 | 14.62 |
| MnK | 50.14 | 25.03 | 3.74 |
| FeK | 7.83 | 3.84 | 10.38 |

**Fig. 12. BS-SEM images and EDX data of sample (1).**

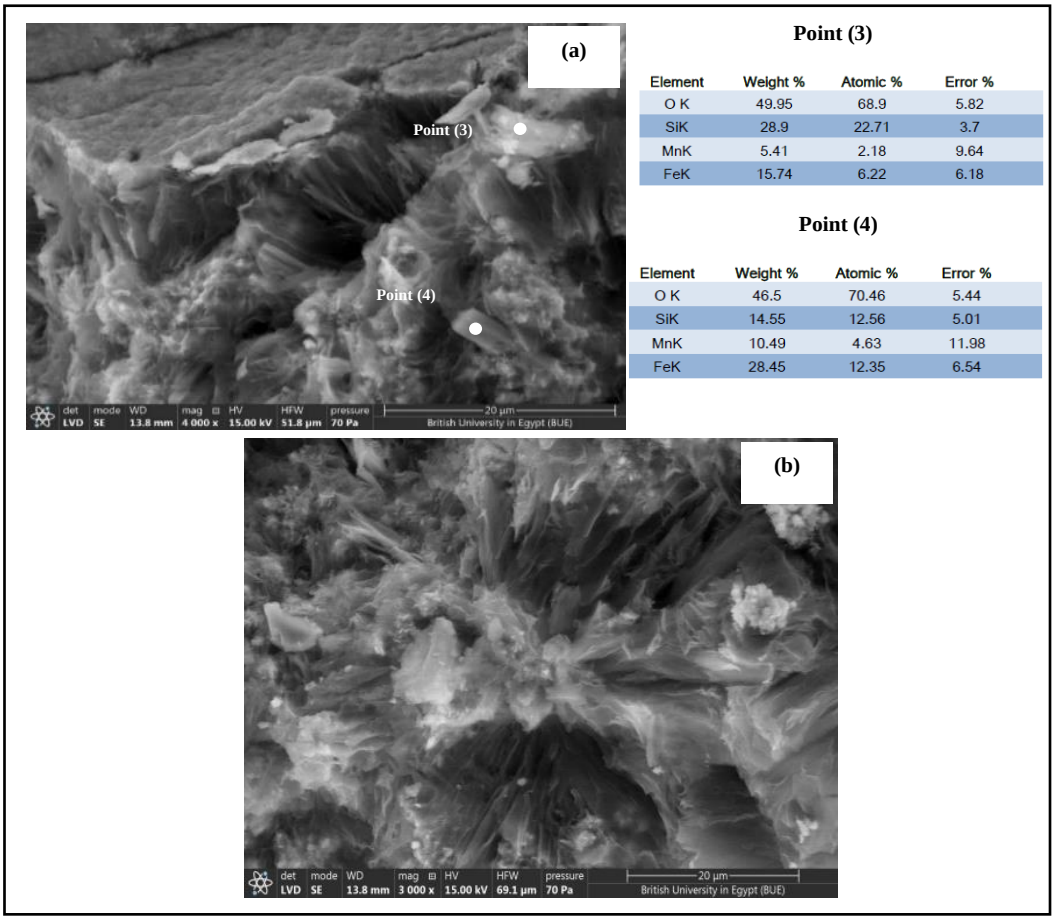


**Point (3)**

| Element | Weight % | Atomic % | Error % |
|---|---|---|---|
| O K | 49.95 | 68.9 | 5.82 |
| SiK | 28.9 | 22.71 | 3.7 |
| MnK | 5.41 | 2.18 | 9.64 |
| FeK | 15.74 | 6.22 | 6.18 |

**Point (4)**

| Element | Weight % | Atomic % | Error % |
|---|---|---|---|
| O K | 46.5 | 70.46 | 5.44 |
| SiK | 14.55 | 12.56 | 5.01 |
| MnK | 10.49 | 4.63 | 11.98 |
| FeK | 28.45 | 12.35 | 6.54 |

**Fig. 13. BS-SEM images and EDX data of sample (2).**

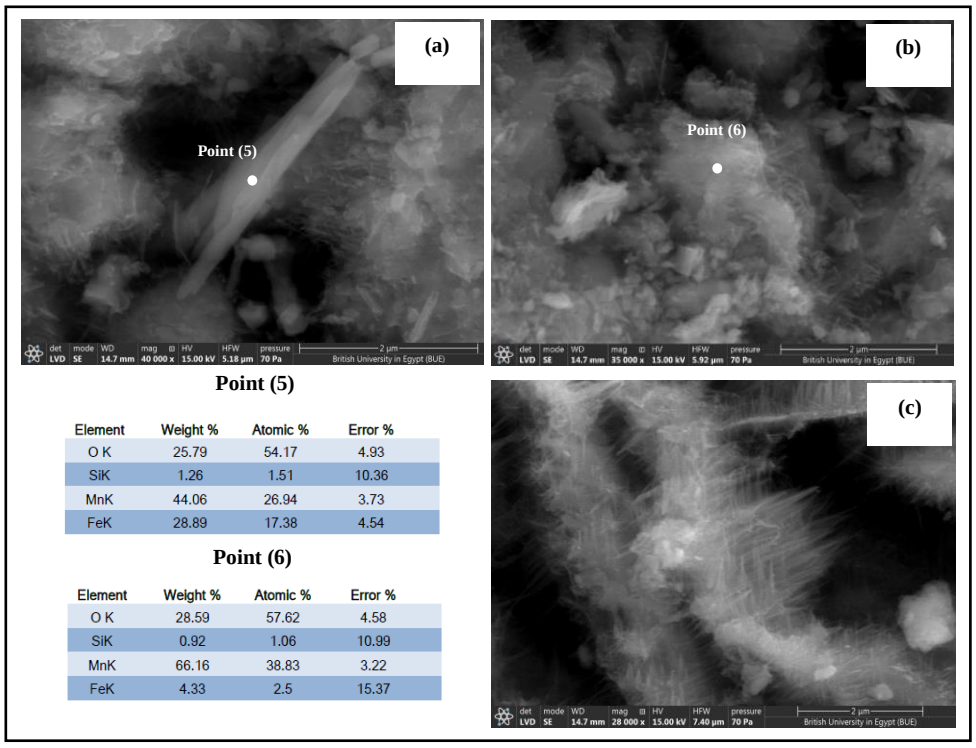


**Point (5)**

| Element | Weight % | Atomic % | Error % |
|---|---|---|---|
| O K | 25.79 | 54.17 | 4.93 |
| SiK | 1.26 | 1.51 | 10.36 |
| MnK | 44.06 | 26.94 | 3.73 |
| FeK | 28.89 | 17.38 | 4.54 |

**Point (6)**

| Element | Weight % | Atomic % | Error % |
|---|---|---|---|
| O K | 28.59 | 57.62 | 4.58 |
| SiK | 0.92 | 1.06 | 10.99 |
| MnK | 66.16 | 38.83 | 3.22 |
| FeK | 4.33 | 2.5 | 15.37 |

**Fig. 14. BS-SEM images and EDX analysis of sample (3).**

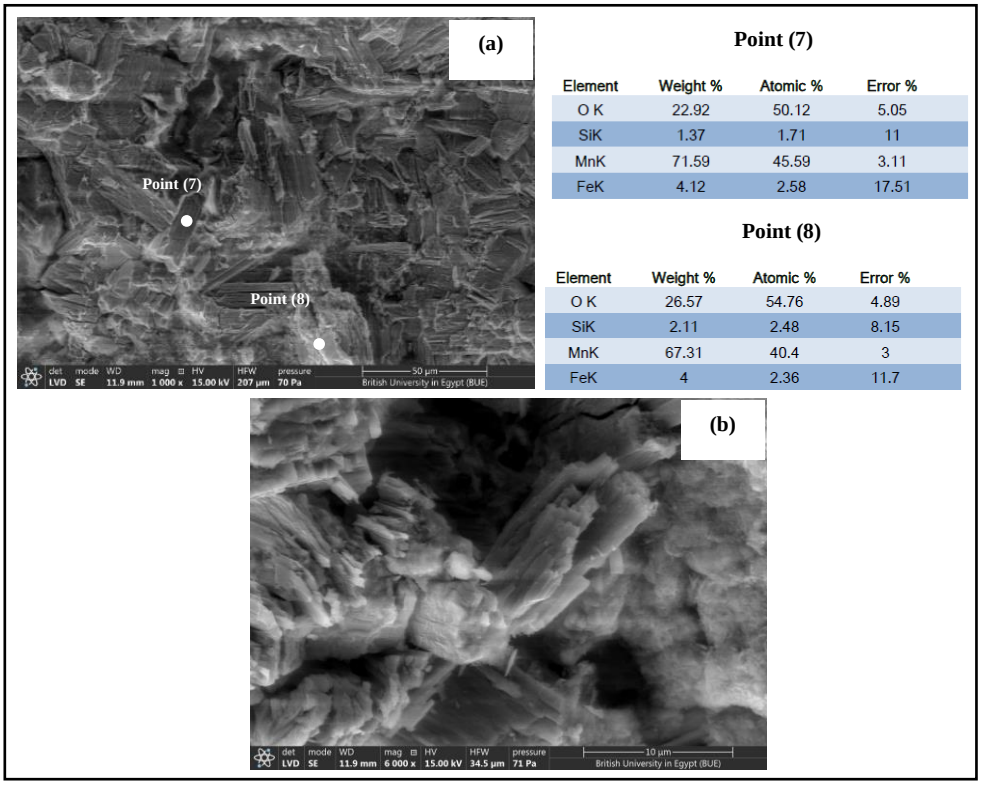


**Point (7)**

| Element | Weight % | Atomic % | Error % |
|---|---|---|---|
| O K | 22.92 | 50.12 | 5.05 |
| SiK | 1.37 | 1.71 | 11 |
| MnK | 71.59 | 45.59 | 3.11 |
| FeK | 4.12 | 2.58 | 17.51 |

**Point (8)**

| Element | Weight % | Atomic % | Error % |
|---|---|---|---|
| O K | 26.57 | 54.76 | 4.89 |
| SiK | 2.11 | 2.48 | 8.15 |
| MnK | 67.31 | 40.4 | 3 |
| FeK | 4 | 2.36 | 11.7 |

**Fig. 15. BS-SEM images and EDX data of sample (4).**

### 3.7. Utilization of manganese ore in manufacturing of the different manganese alloys

According to Sully (1955) and Abd El-Gawad et al (2014), the manganese ores with more than 35% Mn and Mn/Fe > 5 (Tan et al, 2004) could be used in the iron and steel industry to produce manganese alloys.

Based on the geochemical studies of the present technological manganese ore samples 1-4, only sample 4 (Mn% = 53.96; Mn/Fe = 6.47) could be classified as suitable commercial grade in manganese alloys production, while the other three samples 1, 2, and 3 (Mn% = 26.26, 43, and 42.88 respectively; Mn/Fe = 0.85, 2.94, and 2.83 respectively) need to be upgraded to match the industrial demands.

Applying the reduction methods on Um Bogma manganese ore is a possible way to upgrade the ore to match the needed qualifications for the production of ferromanganese alloys (Fahim et al, 2013) and silicon-manganese alloys (El-Faramawy et al, 2022).

## 4. Conclusions

The integration of the data obtained from the various analytical laboratory techniques led to the following findings:

- The studied technological manganese ore samples are composed of varying proportions pyrolusite (26% - 85.9%), hausmannite (18.5%), and hematite (6.5% – 24.2%) as oxide minerals. However, the hydroxide minerals are manganite (4.1 – 66.7%) and goethite (17.1 – 17.6%). The silicate mineral is only quartz (10.4 – 16%).
- Based on the Mn and Fe contents, the samples could be classified into manganiferous iron ore (sample 1; Mn% = 26.26 wt.%) and manganese ore (samples 2, 3, and 4; Mn% = 43%, 42.88%, and 55.695 respectively). As the manganese percentage increases, the iron percentage decreases proportionally.
- Two main textures are recorded in these samples. The first, pyrolusite exists as interlocking crystals and aggregates disseminated in a groundmass made up of hematite and goethite (sample 1). The second microfabric characterizes the rest of the samples and is characterized by the presence of separated islands of Mn-dominated granular patches set in a groundmass composed of hematite and goethite.
- Based on the textural, mineral, and chemical composition of the studied samples, the followings could be concluded:
    1. Sample (1) is not potential to be processed for Mn-content upgrade mainly due to its lowest manganese content (33.93 wt.%) in addition to the interlocking growth of the metallic minerals (pyrolusite and hematite).
    2. Although sample (4) has the maximum MnO content (69.37 wt.%), however, it exists mainly in the form of the manganite (66.7 %) instead of pyrolusite. Accordingly, this sample represents an ore that is not suitable for mineral beneficiation, because it has manganite as the main Mn mineral instead of pyrolusite, which will not be representative of the four samples.
    3. Samples (2) and (3) have almost similar MnO content (55.55% and 55.4 wt.%; respectively). However, sample (3) has a higher potentiality for upgrading by applying different mineral processing mainly due to its granular textural fabric. In addition, this sample consists of pyrolusite (85.9 %) and hematite (10 %), an association that is potential for

processing. On the contrary, sample (2) has a non-uniform microfabric (random-sized patches of Mn minerals between Fe minerals) and a complicated mineral composition (pyrolusite, hausmannite, hematite, goethite, and quartz). This demands additional mineral processing facilities and costs.

**Ethics approval and consent to participate**: This article does not contain any studies with human participants or animals performed by any of the authors.

**Consent for publication**: All authors declare their consent for publication.

**Conflicts of Interest:** The author declares no conflict of interest.

**Contribution of Authors:** All authors shared in writing, editing and revising the MS and agree to its publication.

## 5. References


Abd El-Gawad, H.H., Ahmed, M.M., El-Hussiny, N.A. and Shalabi, M.E.H. (2014) Reduction of Low Grade Egyptian Manganese Ore via Hydrogen at 800˚C - 950˚C. Open Access Library Journal, 1: e427.

Araffa, A. S., Rabeh, T. T., Mousa, E. A., Abdel Nabi, H., & Al Deep, M. (2020). Integrated geophysical investigation for mapping of manganese-iron deposits at Wadi Al Sahu area, Sinai, Egypt-a case study. Arabian Journal of Geosciences 13: 823

Craig J. R. & Vaughan D. J (1994). Ore Microscopy and ore petrography. Second edition. Wiley inter-science publication. John Wiley & Sons, Inc.

Chukanov, N. V., (2014) Infrared spectra of mineral species: Extended library, Springer Geochemistry/Mineralogy

El Shazly, E. M., & Saleeb, G. S. (1959). Contributions to the mineralogy of Egyptian manganese deposits. In Economic Geology (Vol. 54).

El-Agami, N. (2000), Sedimentary Origin of the Mn-Fe Ore of Um Bogma, Southwest Sinai: Geochemical and Paleomagnetic Evidence, Economic Geology. Vol. 95, pp. 607–620.

El-Anwar, E. A. A. (2014). Composition and origin of the dolostones of Um Bogma Formation, Lower Carboniferous, West Central Sinai, Egypt. Carbonates and Evaporites, 29(3), 239–250.

El-Aref, M, Abdel-Rahman,Y., Zoheir,B., Surour,A., Helmy,H., Abdelnasser, A., Ahmed,A.H. Ibrahim,M.E. (2020), Mineral Resources in Egypt (I): Metallic Ores, Egyptian Manganese Deposits, Springer Nature Switzerland AG. Chapter 14.9.

El-Faramawy, H., Eissa, M., Ghali, S.N., Mattar, T., Ahmed, A., El-Fawakhry, M., and Kotb, E.M. (2022) Silicomanganese alloy from rich manganese slag produced from Egyptian low-grade manganese ore. Journal of the Southern African Institute of Mining and Metallurgy, vol. 122, no. 1, pp. 5-14

El-Hussiny, N. A., Abd El-Gawad, H. H., Mohamed, F. M., & Shalabi, M. E. H. (2016). Reduction low grade Egyptian manganese ore by carbon of coke breeze in the form pellets. International Journal of Scientific & Engineering Research, Volume 7, Issue 1.

El-Shafei, S., Ramadan, F., Essawy, M., Henaish, A., & Nabawy, B. (2022). Geology, mineralogy, and geochemistry of manganese ore deposits of the Um Bogma Formation, south-western Sinai, Egypt: Genesis implications. Mining of Mineral Deposits, 16(3), 86–95.

Fahim, M. S., El Faramawy, H., Ahmed, A. M., Ghali, S. N., & Kandil, A. E. H. T. (2013). Characterization of Egyptian Manganese Ores for Production of High Carbon Ferromanganese. Journal of Minerals and Materials Characterization and Engineering, 01(02), 68–74. https://doi.org/10.4236/jmmce.2013.12013

Gindy, A. R., (1961) On the radioactivity and origin of the manganese-iron deposits of west central Sinai. Egypt Acad Sci 16:71–86

Johnson, A.G. and Mccartney, W.C. 1965. Manganese occurrences in Canada. Geological Survey of Canada, Paper 64-37, p. 35–41.

Khalifa, I. H., & Seif, R. A. (2014). Geochemistry of manganese-iron ores at Um Bogma area, west central Sinai, Egypt. International Journal of Advanced Scientific and Technical Research Issue, 4, volume 6.

Kora, M. (1984) The Paleozoic outcrops of Um Bogma area, Sinai: Ph.D. thesis, Monsoura Univ., Egypt, p.280

Kora, M., El Shahat, A., & Abu Shabana, M. (1994). Lithostratigraphy of the manganese-bearing Urn Bogma Formation, west-central Sinai, Egypt. In Journal of African Earth Sciences. Vol. 18, Issue 2. No. 2, pp. 151-162.

Kordi, M., Morad, S., Turner, B., & Salem, A. M. K. (2017). Sequence stratigraphic controls on formation of dolomite: Insights from the Carboniferous Um Bogma Formation, Sinai-Egypt. Journal of Petroleum Science and Engineering, 149, 531–539.

Liu, B., Zhang, Y., Lu, M., Su, Z., Li, G., & Jiang, T. (2019). Extraction and separation of manganese and iron from ferruginous manganese ores: A review. In Minerals Engineering. Vol. 131, pp. 286–303.

Long, Y., Ruan, L., Lv, X., Lv, Y., Su, J., & Wen, Y. (2015). TG-FTIR analysis of pyrolusite reduction by major biomass components. Chinese Journal of

Chemical Engineering, 23(10), 1691–1697. https://doi.org/10.1016/j.cjche.2015.08.028.

Magaritz M, Brenner IB (1979) The geochemistry of a lenticular manganese-ore deposit (Um Bogma, Southern Sinai). Mineral. Deposita 14:1–13.

Mart, J., and Sass, E., (1972) Geology and origin of the manganese ore of Urn Bogma. Sinai. Econ Geol 67:145–15.

Nakhla, F. M., and Shehata M. R. N., (1963) Mineralogy of some manganese iron ores from west central Sinai, Egypt: N-JbMiner., Abh. Vol. 99, N.3, pp. 277–294

Pracejus, B. (2015) The ore minerals under the microscope. Second Edition. Atlases in Geosciences. ElSEVIER

Saad, N. A., Zidan, B. I., & Khalil, K. I. (1994). Geochemistry and origin of the manganese deposits in the Um Bogma region, west central Sinai, Egypt. In Journal of African Earth Sciences. Vol. 19, Issue 2.

Salem, I. A., El-Shibiny, N. H., & Monsef, M. A. (2016). Mineralogical and Geochemical Studies on Manganese Deposits at Abu Ghusun Area, South-Eastern Desert, Egypt. Journal of Geography and Earth Sciences, 4 (2).

Shaaban, M. N., Holail, H. M., Sedeik, K. N., & Rashed, M. A. (2005). Multiple dolomitization events of the Lower Carboniferous Um Bogma Formation, west central Sinai, Egypt. Carbonates and Evaporites, v. 20, no. 2, p. 107-115.

Singh, V., Chakraborty, T., & Tripathy, S. K. (2020). A Review of Low-Grade Manganese Ore Upgradation Processes. In Mineral Processing and Extractive Metallurgy Review. Vol. 41, Issue 6, pp. 417–438.

Song, J., Liu, M., Ma, X., Tian, Q., Feng, J., Zhong, X., Duan, F., (2023) Thermal decomposition behavior and computational analysis of alpha and beta manganese dioxide nanorods. Journal of Alloys and Compounds, Volume 962.

Sully, A.H. (1955) Manganese. Academic Press, New York, 4.

Tan, Z.Z., Mei, G.G., Li, W.J., Zeng, K.X., Liang, R.T., Zeng, X.B., (2004) Metallurgy of Manganese. Central South University Press, Changsha, China (in Chinese).

# توصيف بعض عينات منجنيز أم بجمة بمنطقة أم بجمة وقابليتها للتركيز والمساهمة في صناعة سبائك المنجنيز

**أحمد جمال مصطفى[١]، وناجي علي عبدالخالق[٢]، وأحمد عبدالمنعم شرف الدين[١]، وعبدالمنعم محمد سلطان[١]، والسيد ربيع حسن[٢]**

[١]قسم الجيولوجيا، كلية العلوم، جامعة عين شمس، القاهرة، مصر

[٢]قسم تركيز وتجميع الخامات، معهد تكنولوجيا الخامات ومعالجتها، مركز بحوث وتطوير الفلزات، حلوان، مصر

في هذا البحث تم عمل دراسة نسيجية ومعدنية وكيميائية بالإضافة إلى السلوك الحراري لعينات تقنية تمثل خام منجنيز منطقة أم بجمة، وذلك باستخدام الطرقة المعملية المختلفة. وتم دراسة النتائج لمعرفة مدى ملائمة تلك العينات للتركيز والمساهمة في صناعة سبائك المنجنيز. وأثبتت النتائج أن معدني البيرولوسيت والمانجانيت هي معادن المنجنيز الرئيسية المكونة للخام، بالإضافة إلى تواجدات متباينة من معادن الهوسمانايت والهيماتايت والجوتايت والكوارتز. وتمت مطابقة نتائج التركيب الكيميائي مع التركيب المعدني. وقد أظهرت العينات أنماط نسيجية مختلفة للمعادن المكونة للخام. وعند تكامل النتائج المعملية تأكد قابلية بعض عينات الخام للتركيز وتحسين الجودة.